*Now at the Centre d'Etudes Nucléaires de Saclay.
†Present address: Physics Department, Case Western Reserve University, Cleveland, Ohio 44106.
‡Present address: The Open University, Bletchley, United Kingdom.
[1]This is a definition slightly different from that used in a previous article; see H. Braun *et al.*, Phys. Rev. D 6, 2311 (1972).
[2]H. Braun, D. Evrard, A. Fridman, J.-P. Gerber, G. Maurer, A. Michalon, B. Schiby, R. Strub, and C. Voltolini, Phys. Rev. D 2, 1212 (1970).
[3]See, for instance, D. Evrard, A. Fridman, and C. Hirshfeld, Nucl. Phys. B14, 699 (1969).
[4]H. Braun, D. Evrard, A. Fridman, J.-P. Gerber, A. Givernaud, R. Kahn, G. Maurer, A. Michalon, B. Schiby, R. Strub, and C. Voltolini, Phys. Rev. D 3, 2572 (1971).
[5]H. Graessler *et al.*, Nucl. Phys. B47, 43 (1972).
[6]K. Boesebeck *et al.*, Nucl. Phys. B40, 39 (1972).
[7]H. Bøggild *et al.*, report submitted to the Fifteenth International High Energy Conference on High Energy Physics, Kiev, 1970 (unpublished).
[8]R. S. Panvini, J. Hanlon, W. H. Sims, J. W. Waters, and T. W. Morris, Nucl. Phys. B39, 538 (1972).
[9]See, for instance, Suh Urk Chung, CERN Report No. CERN 71-8, 1971 (unpublished).
[10]See, for instance, H. C. Hsiung, E. Coleman, B. Roe, D. Sinclair, and J. Vander Velde, Phys. Rev. Lett. 21, 187 (1968).
[11]H. Satz, Phys. Lett. 32B, 380 (1970).
[12]D. Dorren, V. Rittenberg, and D. Yaffe, Nucl. Phys. B30, 306 (1971).
[13]Elastic $\bar{p}d$ scattering at 5.55-GeV/c incident momentum, H. Braun, A. Fridman, E. Jegham, P. Juillot, J. A. Malko, C. Voltolini, G. R. Charlton, W. A. Cooper, and B. Musgrave, Nucl. Phys. B54, 61 (1973).
[14]See, for instance, J. V. Beaupré *et al.*, Nucl. Phys. B47, 51 (1972).
[15]G. Cohen-Tannoudji, J. M. Drouffe, P. Moussa, and R. Reshanski, Phys. Lett. 33B, 183 (1970).

PHYSICAL REVIEW D VOLUME 8, NUMBER 9 1 NOVEMBER 1973

Study of Λ^0 and $\bar{\Lambda}^0$ Final States Produced in 12.7-GeV/c K^+p Interactions*

D. Cohen,† T. Ferbel,‡ P. Slattery, and S. Stone§
Department of Physics and Astronomy, University of Rochester, Rochester, New York 14627
(Received 4 April 1973)

We investigate highly constrained final states involving the production of Λ^0 and $\bar{\Lambda}^0$ particles in K^+p interactions at 12.7 GeV/c. We show that Λ^0 production appears to proceed dominantly through processes which can be regarded as the fragmentation of the target, while $\bar{\Lambda}^0$ production appears to result mainly from beam fragmentation.

INTRODUCTION

In a previous publication concerning inclusive Λ^0 and $\bar{\Lambda}^0$ production in K^+p interactions,[1] we observed that Λ^0 hyperons are produced mainly backward in the center-of-mass system and can thus be regarded as remnants of the breakup of the target proton; $\bar{\Lambda}^0$ antihyperons, on the other hand, are produced mainly forward in this system and conversely can be regarded as resulting from the breakup of the incident K^+ meson. Here we report on the characteristics observed for Λ^0 and $\bar{\Lambda}^0$ particles studied in exclusive final states produced in a 10-event/μb exposure of the BNL 80-in. hydrogen bubble chamber to 12.7-GeV/c K^+ mesons.[2] We consider the following reactions:

$$K^+p \to \Lambda^0 K^+ K^+, \tag{1}$$

$$K^+p \to \Sigma^0 K^+ K^+ \searrow \Lambda^0\gamma, \tag{2}$$

$$K^+p \to \Lambda^0 K^+ K^+ \pi^+\pi^-, \tag{3}$$

$$K^+p \to \Sigma^0 K^+ K^+ \pi^+\pi^- \searrow \Lambda^0\gamma, \tag{4}$$

$$K^+p \to \Lambda^0 K^+ K^+ K^+ K^-, \tag{5}$$

$$K^+p \to \Lambda^0 K^+ \pi^+ K_S^0, \tag{6}$$

$$K^+p \to \Sigma^0 K^+ \pi^+ K_S^0 \searrow \Lambda^0\gamma, \tag{7}$$

$$K^+p \to \Lambda^0 K^+ K^+ \pi^0, \tag{8}$$

$$K^+p \to \bar{\Lambda}^0 ppp, \tag{9}$$

$$K^+p \to \bar{\Sigma}^0 ppp \searrow \bar{\Lambda}^0\gamma, \tag{10}$$

$$K^+p \to \bar{\Lambda}^0 ppp\pi^+\pi^-, \tag{11}$$

$$K^+p \to \bar{\Sigma}^0 ppp\pi^+\pi^- \searrow \bar{\Lambda}^0\gamma, \tag{12}$$

$$K^+p \to \bar{\Lambda}^0 ppp\pi^0, \tag{13}$$

$$K^+p \to \bar{\Lambda}^0 pn\pi^+. \tag{14}$$

TABLE I. Topological cross sections for final states involving neutral strange-particle decays.

	Cross section [a]		
	K^0	Λ^0	$\bar{\Lambda}^0$
Total	6.03 ± 0.5 mb	438 ± 40 μb	150 ± 15 μb
2-prong+vee	2.55 ± 0.2 mb	172 ± 18 μb	97 ± 10 μb
4-prong+vee	2.41 ± 0.2 mb	130 ± 13 μb	34 ± 4 μb
6-prong+vee	670 ± 100 μb	30 ± 12 μb	<5 μb
2-prong+2 vee	251 ± 25 μb	48 ± 8 μb	7 ± 4 μb
4-prong+2 vee	130 ± 15 μb	29 ± 6 μb	<3 μb

[a] For the 2-vee topologies each event contributes twice to the above table. The Λ^0 ($\bar{\Lambda}^0$) cross section contains the Σ^0 ($\bar{\Sigma}^0$) contribution.

The film was scanned twice for any events with neutral strange-particle decays (vees) associated with a production vertex. These events were subsequently measured and processed through the TVGP-SQUAW analysis programs. Topological cross sections for final states involving visible neutral strange-particle decays are presented in Table I. These cross sections have been corrected for scanning losses, for escape probabilities, and for neutral decay modes not observed in the bubble chamber.[3] Cross sections for reactions (1)–(14) are presented in Tables II and III. We note that, in general, Λ^0 ($\bar{\Lambda}^0$) production cross sections are larger than Σ^0 ($\bar{\Sigma}^0$) production cross sections for similar final states. We proceed to discuss the production characteristics observed for the more constrained reactions (1)–(7) and (9)–(12).

TABLE II. Cross sections for some exclusive reactions with a final state Λ^0 or Σ^0.

Reaction	Number of events	Cross section (μb) [a]
$K^+p \to \Lambda^0K^+K^+$	61	12.3 ± 2.1
$K^+p \to \Sigma^0K^+K^+$	7	1.3 ± 0.9
$K^+p \to \Lambda^0K^+K^+\pi^+\pi^-$	88	18.2 ± 2.7
$K^+p \to \Sigma^0K^+K^+\pi^+\pi^-$	26	5.9 ± 1.3
$K^+p \to \Lambda^0K^+K^+K^+K^-$	17	3.6 ± 0.9
$K^+p \to \Lambda^0K^+\pi^+K^0$	33	25 ± 7
$K^+p \to \Sigma^0K^+\pi^+K^0$	12	9 ± 3
$K^+p \to \Lambda^0K^+K^+\pi^0$	10	15 ± 8

[a] All cross sections have been corrected for escape probabilities and for unobservable decay channels. The cross sections involving a K^0 in the final state assume equal production of K_L^0 and K_S^0.

TABLE III. Cross sections for some exclusive reactions with a final state $\bar{\Lambda}^0$ or $\bar{\Sigma}^0$.

Reaction	Number of events	Cross section (μb) [a]
$K^+p \to \bar{\Lambda}^0pp$	35	8.2 ± 1.6
$K^+p \to \bar{\Sigma}^0pp$	7	1.6 ± 0.8
$K^+p \to \bar{\Lambda}^0pp\pi^+\pi^-$	56	12.5 ± 2.5
$K^+p \to \bar{\Sigma}^0pp\pi^+\pi^-$	3	0.6 ± 0.4
$K^+p \to \bar{\Lambda}^0pp\pi^0$	33	8.8 ± 1.6
$K^+p \to \bar{\Lambda}^0pn\pi^+$	67	15.7 ± 2.7

[a] All cross sections have been corrected for escape probabilities and for unobservable decay channels.

THE REACTIONS $K^+p \to \Lambda^0K^+K^+$ AND $K^+p \to \Sigma^0K^+K^+$

A plot of the production cross section versus incident beam momentum (P_{lab}) for the reaction $K^+p \to \Lambda^0K^+K^+$ is shown in Fig. 1.[4] We note that the production cross section for this channel appears to be falling very slowly with increasing P_{lab} ($\sim P_{lab}^{-1/3}$).

We can examine the production characteristics of the final-state particles in reactions (1) and (2), denoting by Y^0 either a Λ^0 or a Σ^0. In Fig. 2 we show the production cosine ($\cos\theta$) in the center-of-mass frame for the Y^0 (Ref. 5); as expected, a sharp backward peak is observed. (The direction of the incident K^+ is taken as positive.) In Fig. 3 we display a scatter plot of $\cos\theta$ for the more forward-outgoing K^+ ($\cos\theta_{Kf}$) versus $\cos\theta$ for the more backward-going K^+ ($\cos\theta_{Kb}$). The sharp forward peak in the $\cos\theta_{Kf}$ distribution indicates that there is always a very fast "beamlike" K^+ associated with each event; it is therefore reasonable to assume that the backward K^+ may result from fragmentation of the proton into a Y^0 and a K^+.

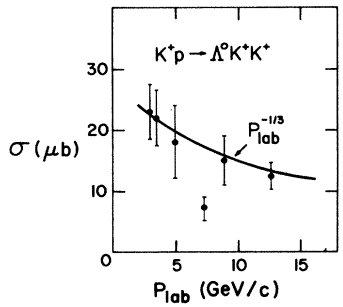

FIG. 1. Cross section for the reaction $K^+p \to \Lambda^0K^+K^+$ as a function of beam momentum.

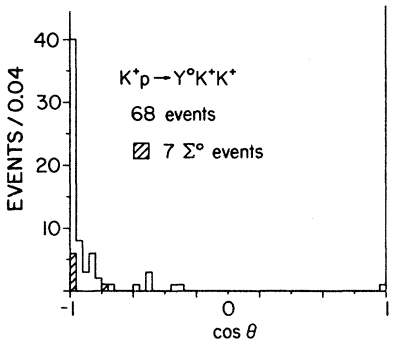

FIG. 2. The center-of-mass cosine for the Y^0 in the $Y^0K^+K^+$ final state. Σ^0 events are cross-hatched.

To further investigate this fragmentation hypothesis, we show in Fig. 4 the Dalitz plot for these reactions; the square of the mass of the Y^0 and K_f^+ is displayed against the square of the mass of the Y^0 and K_b^+. A definite enhancement appears in the region of low $Y^0K_b^+$ mass. This sort of low-mass peak is characteristic of diffractive processes[6]; we thus conclude that, on the basis of the weak energy dependence and these observed production characteristics, reactions (1) and (2) are dominated by a diffractive mechanism.

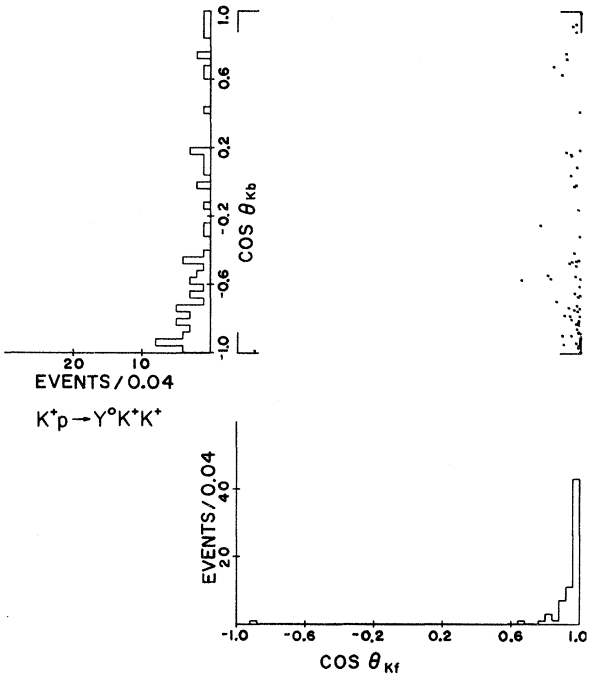

FIG. 3. The center-of-mass cosine of the more forward K^+ ($\cos\theta_{K_f}$) versus the center-of-mass cosine of the more backward K^+ ($\cos\theta_{K_b}$) for the $Y^0K^+K^+$ final state.

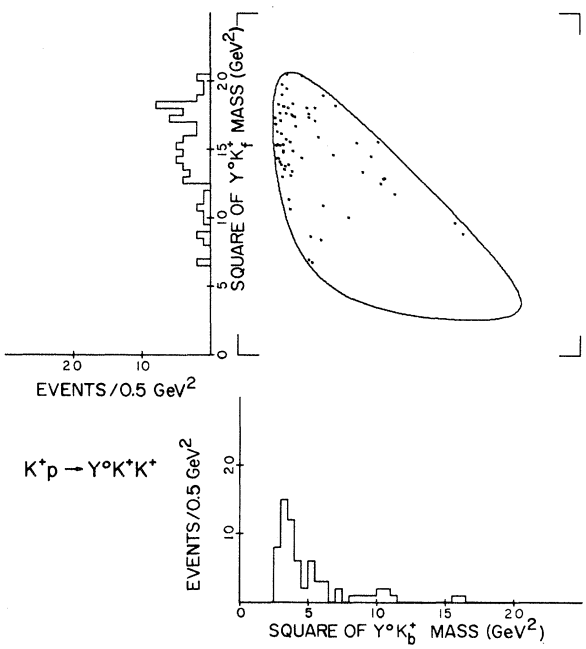

FIG. 4. Dalitz plot for the $Y^0K^+K^+$ final state.

By assuming SU(3) symmetry and the diffractive (Pomeranchukon-exchange) diagram shown in Fig. 5, we can obtain a prediction for the ratio

$$R = \frac{\sigma(K^+p \to \Sigma^0K^+K^+)}{\sigma(K^+p \to \Lambda^0K^+K^+)},$$

which we have experimentally determined to be $(10 \pm 8)\%$. If the Pomeranchukon is taken as an SU(3) singlet, this calculation involves the coupling of two octets (meson + baryon) to form a third octet (baryon). The coupling between the two octets may be either symmetric (D) or antisymmetric (F). For pure D coupling R is $\frac{1}{3}$, while for pure F coupling R is 3. If for the intermediate baryon we use the measured values of D/F for the baryon octet found in weak interactions,[7] we predict $R = (23 \pm 2)\%$. Our results are hence consistent with the coupling expected from the measured D/F ratio, but are not inconsistent with pure D coupling. Pure F coupling is clearly not in ac-

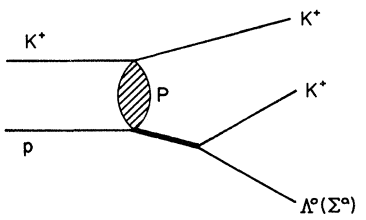

FIG. 5. Pomeranchukon exchange diagram for $K^+p \to Y^0K^+K^+$.

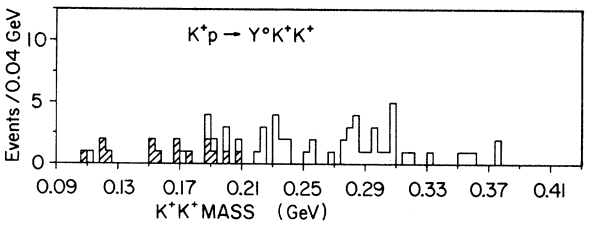

FIG. 6. K^+K^+ mass for the $Y^0K^+K^+$ final state. The cross-hatched events have $\cos\theta_{K_f} > \cos\theta_{K_b} > 0$.

cord with our data.

In addition to events which are produced by the dominant diffractive process, we can discern another class of events in reactions (1) and (2). These events do not have low $Y^0K_b^+$ mass and have two fast outgoing K^+ mesons in the final state. In Fig. 6 we show the mass of the two K^+ mesons; the shaded events have $\cos\theta > 0$ for both K^+. We see that these events favor small K^+K^+ mass, and may result from a meson-exchange process.

THE REACTIONS $K^+p \to \Lambda^0K^+K^+\pi^+\pi^-$ AND $K^+p \to \Sigma^0K^+K^+\pi^+\pi^-$

We examine the production characteristics of reactions (3) and (4) combined. In Fig. 7 we show the distribution in $\cos\theta$ for the Y^0; a backward peak, similar to the one observed in reactions (1) and (2), is also evident here. In Fig. 8 we plot $\cos\theta$ of the more forward-outgoing K^+ ($\cos\theta_{Kf}$) versus $\cos\theta$ of the more backward-going K^+ ($\cos\theta_{Kb}$); again we find that there usually is a fast forward K^+ associated with a slower backward K^+. Plotting in Fig. 9(a) the invariant mass of K_b^+ and the Y^0, we observe a low-mass enhancement (shaded events) which is wider than the corresponding enhancement in reactions (1) and (2). In Fig. 9(b) we look for evidence of diffractive production in these final states by examining the mass recoiling from K_f^+. We also search for a Q type of enhancement[6] in the $K^+\pi^+\pi^-$ mass spectrum [Fig. 9(c)]. Although the cross section appears to be large for smaller values of $YK_b^+\pi^+\pi^-$ mass, we find no evidence for any significant enhancements in these mass spectra. The only resonance production in these final states involves the $K^{*0}(890)$ [Fig. 9(d)]; it is interesting to note that $K^*(890)$ production is mostly associated with K_b^+ and, consequently, mainly with the low-mass portion of the $YK_b^+\pi^+\pi^-$ mass spectrum.

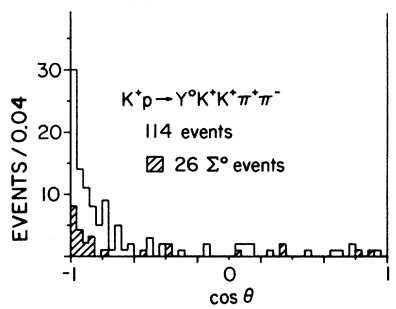

FIG. 7. The center-of-mass cosine of the Y^0 for the $Y^0K^+K^+\pi^+\pi^-$ final state. Σ^0 events are cross-hatched.

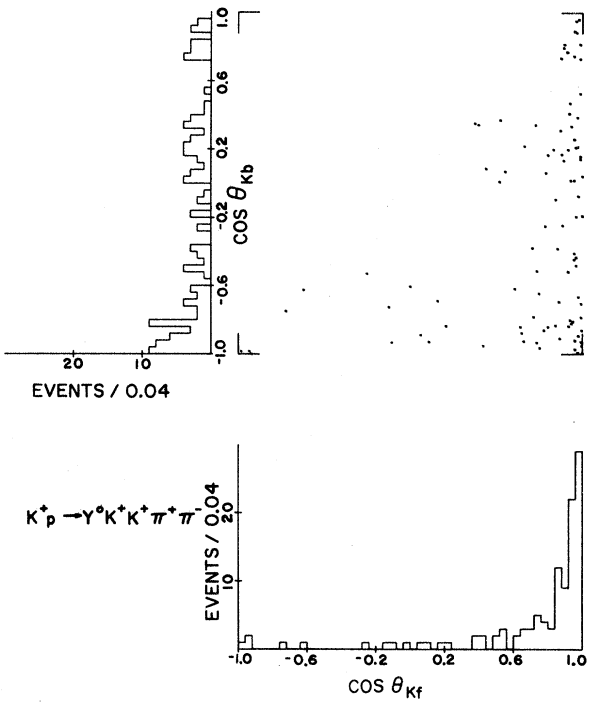

FIG. 8. The center-of-mass cosine of the more forward K^+ ($\cos\theta_{K_f}$) versus the center-of-mass cosine of the more backward K^+ ($\cos\theta_{K_b}$) for the $Y^0K^+K^+\pi^+\pi^-$ final state.

THE REACTION $K^+p \to \Lambda^0K^+K^+K^+K^-$

In this reaction there is some evidence for a low-mass $\Lambda^0K_b^+$ enhancement [K_b^+ now refers to the K^+ produced most backward in the center-of-mass system; see Fig. 10(a)]. A small ϕ^0 signal is also observed in this final state [Fig. 10(b)]. We do not find any compelling evidence for diffractive production processes in the other mass spectra for this channel (see Fig. 11); however, it should be pointed out that in reactions (3)–(5) we are dealing with dissociation into rather massive systems at moderate beam energies and, consequently, kinematic restriction tends to mask those characteristics observed in low-mass dissociation processes.

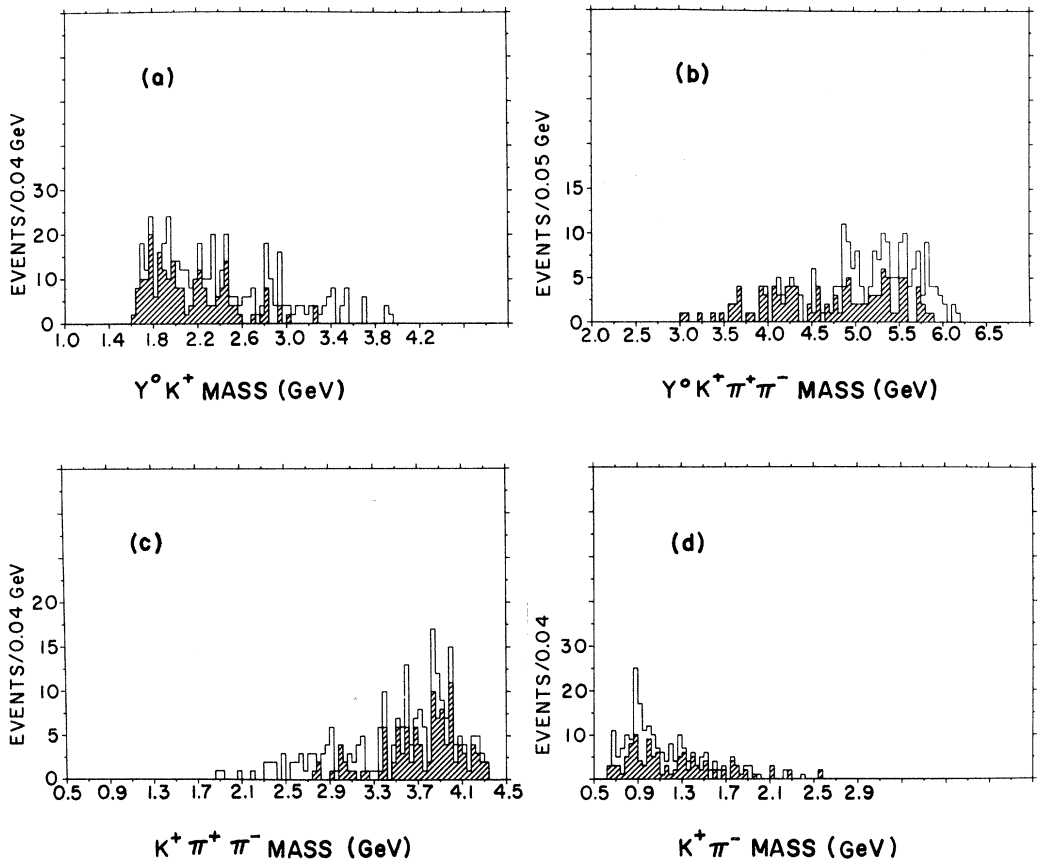

FIG. 9. Mass spectra for the $Y^0K^+K^+\pi^+\pi^-$ final state. (a) Y^0K^+ mass; the cross-hatched events are the $Y^0K_b^+$ mass combinations; (b) $Y^0K^+\pi^+\pi^-$ mass; the cross-hatched events are the $Y^0K_b^+\pi^+\pi^-$ mass combinations; (c) $K^+\pi^+\pi^-$ mass; the cross-hatched events are the $K_f^+\pi^+\pi^-$ mass combinations; (d) $K^+\pi^-$ mass; the cross-hatched events are the $K_f^+\pi^-$ mass combinations.

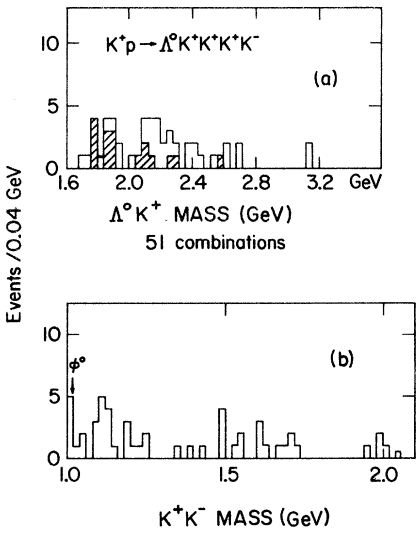

FIG. 10. Mass spectra for the $\Lambda^0K^+K^+K^+K^-$ final state. (a) Λ^0K^+ mass; the cross-hatched events are the $\Lambda^0K_b^+$ mass combinations; (b) K^+K^- mass.

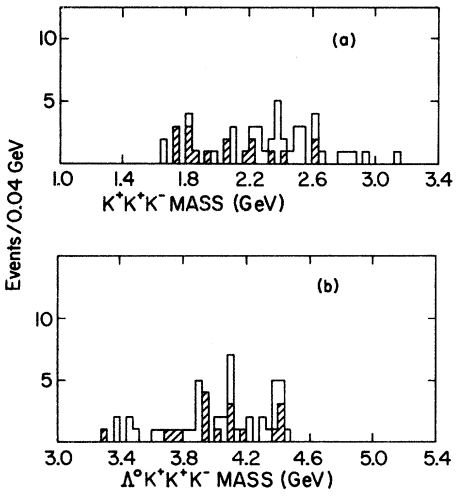

FIG. 11. Mass spectra for the $\Lambda^0K^+K^+K^-$ final state. (a) $K^+K^+K^-$ mass; cross-hatched events contain the combination opposite K_b^+; (b) $\Lambda^0K^+K^+K^-$ mass; cross-hatched events contain the combination opposite K_f^+.

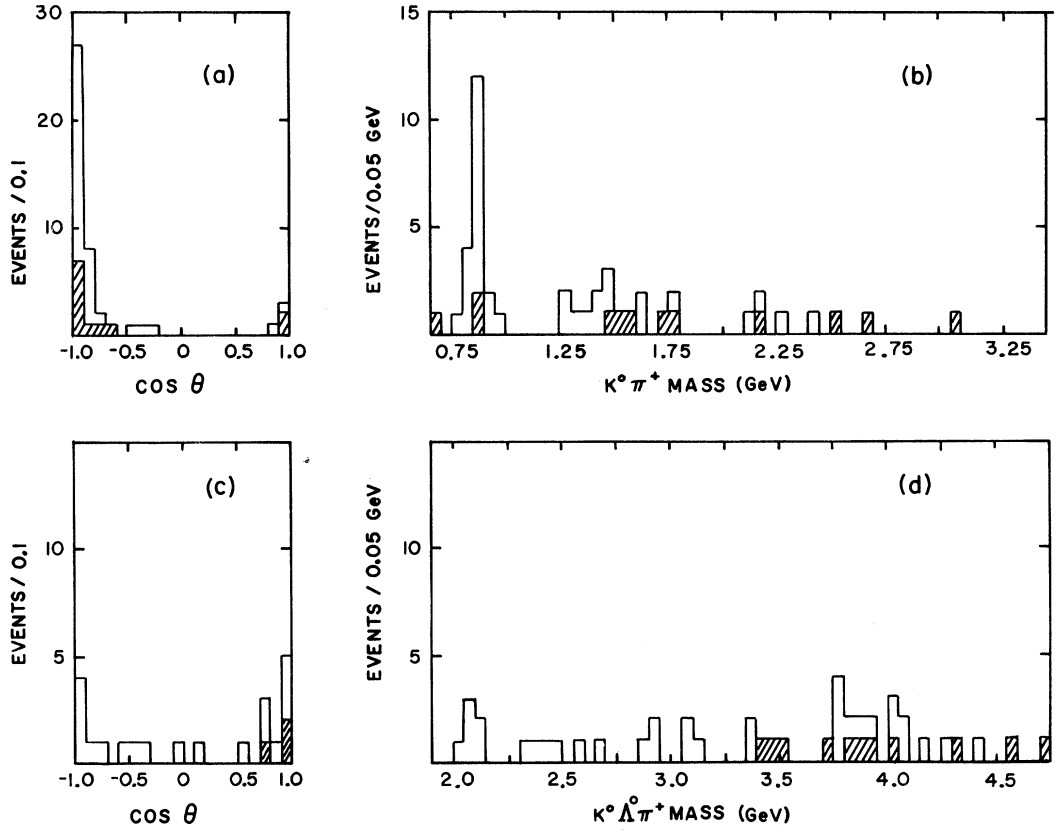

FIG. 12. Distributions for the $Y^0K^+\pi^+K^0$ final state; the Σ^0 events are cross-hatched. (a) Center-of-mass cosine of the Y^0; (b) $K^0\pi^+$ mass; (c) center-of-mass cosine of the $K^{*+}(890)$; (d) $Y^0K^0\pi^+$ mass.

THE REACTIONS $K^+p \to \Lambda^0K^+\pi^+K^0$ AND $K^+p \to \Sigma^0K^+\pi^+K^0$

We considered for analysis only those events with a detected Λ^0 and K_S^0 in the final state. In Fig. 12(a) we show $\cos\theta$ for the Y^0, and note that it is also backward-peaked. The only statistically significant resonance production in these channels is the $K^*(890)$ [Fig. 12(b)], which appears to be associated with both the beam and the target particles [Fig. 12(c)]. We do not find any compelling evidence for the dominance of diffractive mechanisms in these reactions [see Fig. 12(d)].

THE REACTIONS $K^+p \to \bar{\Lambda}^0pp$ AND $K^+ \to \bar{\Sigma}^0pp$

The cross section for reaction (9) as a function of incident beam momentum is shown in Fig. 13.[8] Although several data points appear to be inconsistent with each other, the cross section appears

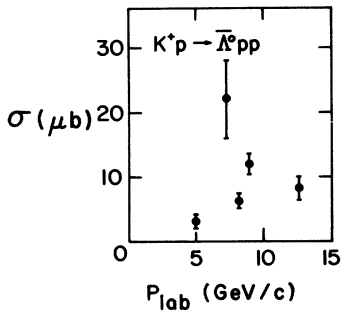

FIG. 13. Cross section for the reaction $K^+p \to \bar{\Lambda}^0pp$ as a function of beam momentum.

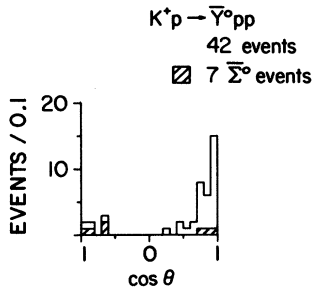

FIG. 14. The center-of-mass cosine of the Y^0 for the $\bar{Y}^0pp$ final state. $\bar{\Sigma}^0$ events are cross-hatched.

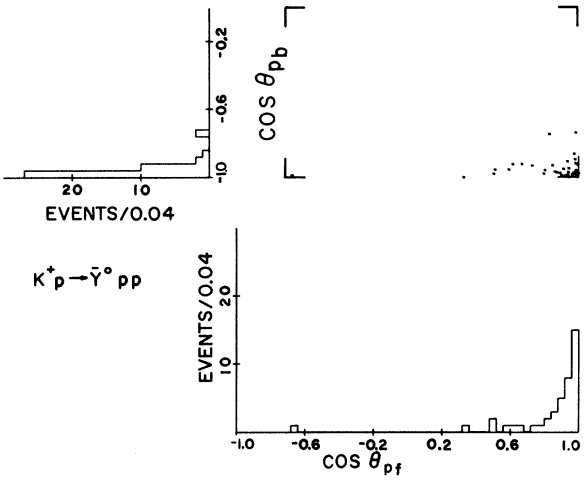

FIG. 15. The center-of-mass cosine of the more forward proton ($\cos\theta_{p_f}$) versus the center-of-mass cosine of the more backward proton ($\cos\theta_{p_b}$) for the $\bar{Y}^0 pp$ final state.

to remain relatively constant over a wide momentum range.

In order to study the production characteristics of reactions (9) and (10), we plot in Fig. 14 the center-of-mass cosine of the $\bar{Y}^0$ ($\bar{\Lambda}^0$ or $\bar{\Sigma}^0$). The distribution in $\cos\theta$ is strongly peaked in the forward direction supporting the contention that the

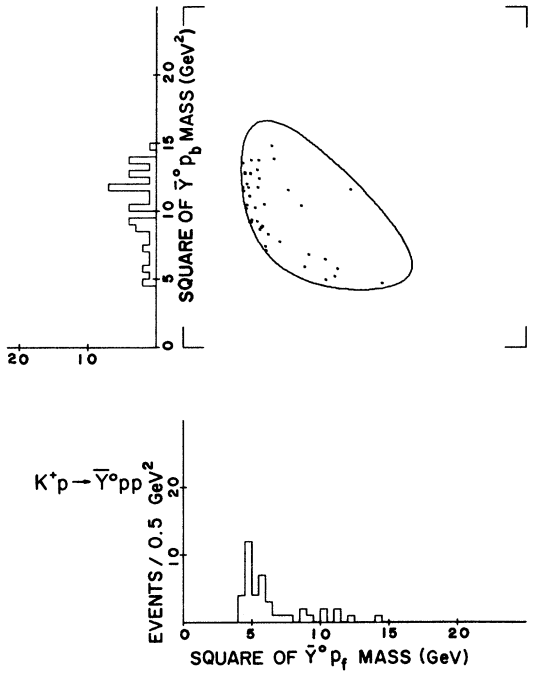

FIG. 16. Dalitz plot for the $\bar{Y}^0 pp$ final state.

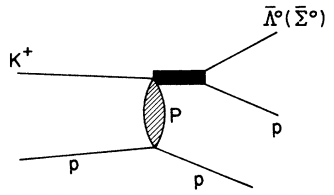

FIG. 17. Pomeranchuckon exchange diagram for the reaction $K^+p \to \bar{Y}^0 pp$.

$\bar{Y}^0$ is mainly a "beamlike" particle. In Fig. 15 we plot the center-of-mass cosine of the more forward proton ($\cos\theta_{p_f}$) versus the center-of-mass cosine of the more backward proton ($\cos\theta_{p_b}$). We see that there is always a beamlike proton and a targetlike proton in the final state. When we consider the Dalitz plot for this reaction [Fig. 16(a)], using the square of the mass of the forward proton and the $\bar{Y}^0$ as one variable and the square of the mass of the $\bar{Y}^0$ and the backward proton as the other, we see a low-mass enhancement in the $\bar{Y}^0 p_f$ mass spectrum.[9] We conclude on the basis of the weak energy dependence and these production characteristics that the low-mass enhancement found in reactions (9) and (10) also results from a diffractive process.

Assuming the diffractive diagram shown in Fig. 17 and SU(3) symmetry, we can predict the expected ratio for

$$R = \frac{\sigma(K^+p \to \bar{\Sigma}^0 pp)}{\sigma(K^+p \to \bar{\Lambda}^0 pp)};$$

we have experimentally determined R to be $(17 \pm 9)\%$. If the K^+ meson has the same C-symmetry properties as the π^0 meson, then, since the C parity of the π^0 is positive, this allows only symmetric (D-type) coupling between the baryon and antibaryon octets. Thus SU(3) predicts that R is 33%, a number just barely consistent with our data.

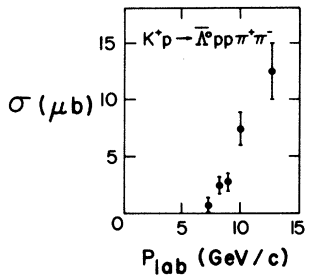

FIG. 18. Cross section for the reaction $K^+p \to \bar{\Lambda}^0 pp\pi^+\pi^-$ as a function of beam momentum.

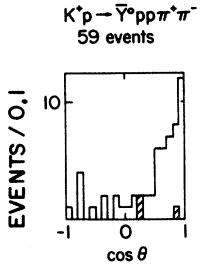

FIG. 19. The center-of-mass cosine of the $\bar{Y}^0$ for the $\bar{Y}^0 p p \pi^+ \pi^-$ final state. $\bar{\Sigma}^0$ events are cross-hatched.

THE REACTIONS $K^+p \to \bar{\Lambda}^0 pp\pi^+\pi^-$ AND $K^+p \to \bar{\Sigma}^0 pp\pi^+\pi^-$

In Fig. 18 we present the cross section for reaction (11) as a function of incident beam momentum.[8,10] This cross section is increasing very rapidly with P_{lab}, approximately doubling from 9 to 13 GeV/c. This is presumably a threshold effect due to the presence of massive particles in the final state.

We consider the production characteristics of the products in reactions (11) and (12), displaying in Fig. 19 the center-of-mass cosine of the $\bar{Y}^0$. The distribution is forward-peaked in the center of mass, as it was for reactions (9) and (10) (Fig. 14). Thus we also consider the $\bar{Y}^0$ to be a beam-

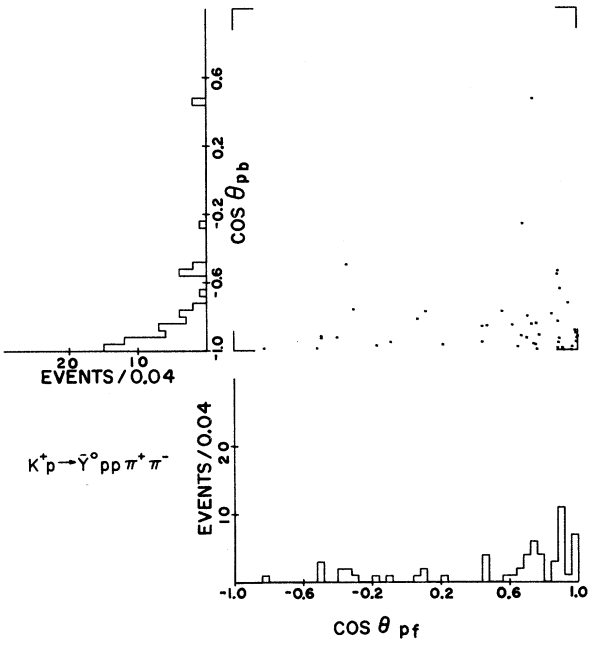

FIG. 20. The center-of-mass cosine of the more forward proton ($\cos\theta_{p_f}$) versus the center-of-mass cosine of the more backward proton ($\cos\theta_{p_b}$) for the $\bar{Y}^0 p p \pi^+ \pi^-$ final state.

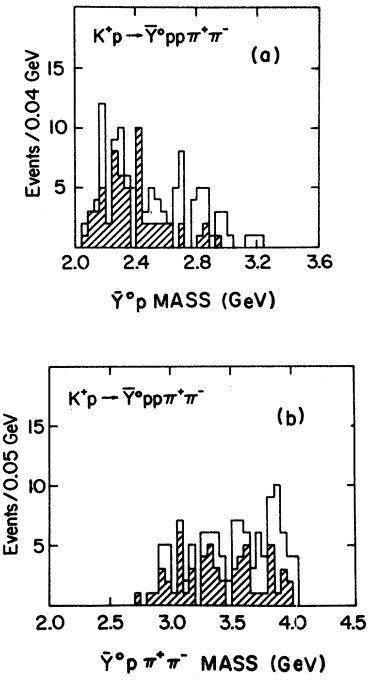

FIG. 21. Mass spectra for the $\bar{Y}^0 p p \pi^+ \pi^-$ final state. (a) $\bar{Y}^0 p$ mass; the cross-hatched events are the $\bar{Y}^0 p_f$ mass combinations; (b) $\bar{Y}^0 p \pi^+ \pi^-$ mass; the cross-hatched events are the $\bar{Y}^0 p_f \pi^+ \pi^-$ mass combinations.

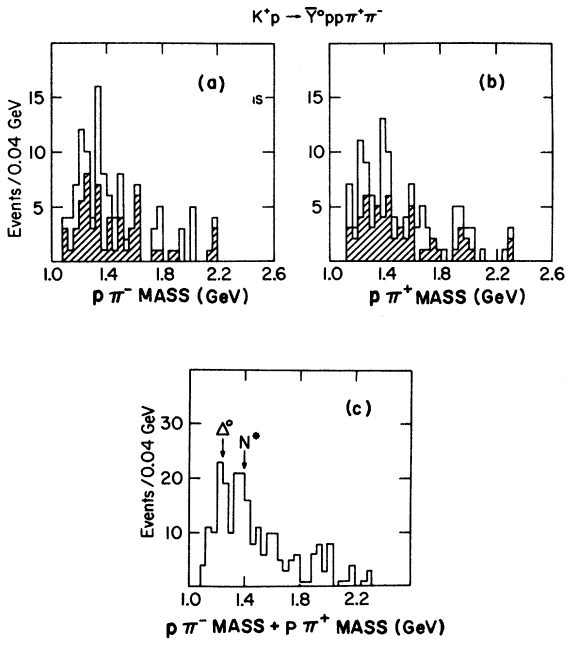

FIG. 22. Mass spectra for the $\bar{Y}^0 p p \pi^+ \pi^-$ final state. (a) $p\pi^-$ mass; the cross-hatched events are the $p_f \pi^-$ mass combinations; (b) $p\pi^+$ mass; the cross-hatched events are the $p_f \pi^+$ mass combinations; (c) sum of the $p\pi^-$ mass and the $p\pi^+$ mass distributions.

like particle in these reactions.

In Fig. 20 we plot the center-of-mass cosine of the two protons in the final state. As before, the more forward proton is denoted as p_f and the more backward as p_b. We see that each event has a beamlike proton and a targetlike proton in the final state.

When we plot the mass of the $\overline{Y}^0$ and beamlike proton [Fig. 21(a)], we observe a low-mass enhancement similar to the one observed in reactions (9) and (10) (Fig. 16). In Fig. 21(b) we search for further evidence for a diffractive production process in these final states by examining the mass recoiling from the targetlike proton (p_b). At the present level of statistics, we do not find any convincing evidence for a diffractive process. We note that some $\Delta^0(1236)$ and $N^*(1470)$ appear to be produced in these data (see Fig. 22).

CONCLUSIONS

We find in these highly constrained final states that Λ^0 hyperons appear to result from the fragmentation of the target proton into a Y^0 and a K-meson system (occasionally with additional mesons). Similarly, $\overline{\Lambda}^0$ hyperons appear to result from the fragmentation of the incident K^+ meson into a $\overline{Y}^0$ and a proton (again occasionally with additional mesons). We have found no evidence, at the level of 5 μb, for the existence of reactions where both the incident K^+ and the target proton fragment simultaneously into $\overline{Y}^0$ and Y^0 systems, respectively.

---

*Research supported by the U. S. Atomic Energy Commission. Computer analysis supported through funds provided by the University of Rochester.

†Presently at Nevis Laboratories, Columbia University, Irvington, N. Y.

‡A. P. Sloan Research Fellow.

§Presently at Vanderbilt University, Nashville, Tenn.

[1]W. Barletta *et al.*, Nucl. Phys. B51, 499 (1973); S. Stone *et al.*, Phys. Rev. D 5, 1621 (1972); S. Stone, Ph.D. thesis, University of Rochester Report No. UR-388, 1972 (unpublished).

[2]For a preliminary study see J. C. Berlinghieri *et al.*, Phys. Lett. 27B, 665 (1968). For a report on Λ^0 and $\overline{\Lambda}^0$ particles produced in final states involving Ξ's, see S. L. Stone *et al.*, Phys. Lett. 32B, 515 (1970).

[3]For more details pertaining to questions of ambiguity and analysis see the thesis of Stone in Ref. 1.

[4]For the 3-, 3.5-, and 5-GeV/c data, see M. Ferro-Luzzi *et al.*, Phys. Lett. 17, 155 (1965). For the 3.5-GeV/c data see also A. R. Erwin *et al.*, Phys. Rev. 149, 1062 (1966). The 7.3-GeV/c data are reported by C. Y. Chien *et al.* [Phys. Lett. 25B, 426 (1967)] and D. J. Mellema [Ph.D. thesis, UCLA, 1970 (unpublished)]. The 9-GeV/c data were communicated to us by A. Firestone.

[5]The angular distributions are uncorrected for escape probability. The weight functions can be described approximately by a quadratic in $\cos\theta$: $1+A\cos\theta+B\cos^2\theta$. For Λ^0, $A\sim 0.19$ and $B\sim 0.22$, while for $\overline{\Lambda}^0$, $A\sim 0.17$ and $B\sim 0.08$. The shapes of the mass spectra are relatively insensitive to the weights.

[6]See, for example, G. L. Kane, in *Phenomenology of Diffractive Reactions,* Lectures at the XII Cracow School of Theoretical Physics, Zakopane, 1972 (unpublished); Rutherford Laboratory Report No. RPP/T/20 (unpublished).

[7]For a measurement of F/D ratio, see N. Barash *et al.*, Phys. Rev. Lett. 19, 181 (1967). See also L. Wolfenstein, in *Proceedings of the International Conference on Elementary Particles, Heidelberg, Germany, 1967,* edited by H. Filthuth (North-Holland, Amsterdam, 1968).

[8]For the 5-GeV/c data see G. Bassompiere *et al.*, Nuovo Cimento 48A, 589 (1967). For the 7.3-GeV/c data see Ref. 5. For the 8.25-GeV/c data see G. Charrière *et al.*, Nucl. Phys. B22, 333 (1970). For the 9-GeV/c data see D. Lissauer *et al.*, Nucl. Phys. B18, 491 (1970).

[9]This enhancement has been discussed by P. F. Slattery [invited talk at the 1971 Austin Meeting of the Division of Particles and Fields of the American Physical Society (unpublished); University of Rochester Report No. UR-322 (unpublished)]; G. Alexander *et al.*, Phys. Rev. Lett. 20, 775 (1968).

[10]K. W. J. Barnam *et al.*, Nucl. Phys. B28, 291 (1971).